How to cite: *Angew. Chem. Int. Ed.* **2025**, *64*, e202507073
doi.org/10.1002/anie.202507073

Slide-ring Gels

Photoresponsive Slide-Ring Gels Enable Modulation of Sliding Dynamics

*Dalila Cafagno, Serena Silvi, Mark W. Tibbitt, and Stefan Mommer**

Abstract: Cyclodextrin-based slide-ring gels (SRGs) have emerged as a promising class of materials owing to their unique topology. Upon mechanical loading, the slidable cross-links of the polymer network freely translocate along the polymer backbone enabling pronounced energy dissipation in the material, which is associated with exceptional ductility and toughness. Despite the critical role of sliding dynamics in defining SRG mechanical properties, attempts to control them have primarily been limited to tuning the overall loading of macrocycles. Further, SRGs that can be triggered via an external stimulus have yet to be reported. In this work, we present light-responsive SRGs based on azobenzene-containing polymers. Reversible photoswitching of the azobenzenes modulates the sliding dynamics of the threaded α-cyclodextrin (α-CD) macrocycles. By using UV–Vis and circular dichroism spectroscopy, we show that α-CDs readily bind to the azobenzenes along the polymer backbone in the *E* configuration. Upon light irradiation, and thus isomerization to the *Z* isomer, the macrocycles no longer interact with the azobenzenes, allowing them to freely translocate along the polymer backbone. As a result of this *E* to *Z* isomerization and difference in sliding dynamics, the mechanical properties of the SRGs reversibly alternate between a stiff and a soft state.

Introduction

Slide-ring gels (SRGs) are hydrogel networks, wherein the crosslinks can freely translocate along the network polymers. This unique topology has rendered polymer materials with fascinating mechanical properties, such as extreme equilibrium swelling, stretchability and toughness.[1,2] Traditional SRGs are prepared by threading macrocycles, such as cyclodextrins (CD),[3,4] crown ethers,[5,6] or pillar[n]arenes,[7,8] onto host polymers to form poly(pseudorotaxanes). To prevent dethreading, the polymer chains are capped with a stopping agent and the distinct macrocycles are chemically linked together to generate networks through figure-of-eight cross-links.[9]

To date, CD-based SRGs are still the most studied class of SRGs, yet the only way to alter ring mobility in these materials is to vary the overall number of threaded rings. While precise control over this number remains challenging, higher CD loadings produced stiffer and more elastic SRGs, while lower coverages generated materials with extreme stretchability and toughness.[4,10,11] Despite previous efforts, reversible and on-demand control of the sliding range in CD-based SRGs has not been realized, mainly because CD macrocycles exhibit the same average binding affinity across the entire polymer backbone. This represents a clear limitation with regard to gaining insights into the slide-ring topology of this class of materials.

The power of controlling sliding dynamics was recently demonstrated by Ghiassinejad et al.,[2] who used metal cation-templated assemblies as an alternative strategy to fabricate SRGs.[12–14] In the presence of Palladium(II), a tetragonal planar complex was formed between the polymer backbone and the threaded macrocycle. In this fixed-ring state, the modulus increased markedly and was independent of frequency, whereas the free-ring state produced a softer gel with extreme stretchability (1600%). To this end, the metal ions introduced a handle to preassemble the cross-linker and a defined binding interaction between the macrocycle and the threaded polymer. This further rendered the SRGs stimuli-responsive (e.g., by varying pH, or ion concentration) and, more importantly, enabled control of the available sliding range. While this chemistry is elegant, it has not been applicable to CD-based SRGs, for which modulating the sliding dynamics remains a challenge.

Inspired by these works, we hypothesized that installing reversible binding moieties along the network backbones would enable similar features in CD-based SRGs. Accordingly, we designed photoswitchable CD-based SRGs supramolecular host–guest interactions that can

---

[*] D. Cafagno, Assoc. Prof. M. W. Tibbitt, Dr. S. Mommer
Department of Mechanical and Process Engineering,
Macromolecular Engineering Laboratory, ETH Zurich,
Sonneggstrasse 3, Zurich 8092, Switzerland
E-mail: smommer@ethz.ch

D. Cafagno, Assoc. Prof. S. Silvi
Dipartimento di Chimica “Giacomo Ciamician”, Università di
Bologna, Via Selmi 2, Bologna, Italy

D. Cafagno
Dipartimento di Chimica, Biologia e Biotecnologia, Università di
Perugia, Via Elce di Sotto 8, Perugia, Italy

Additional supporting information can be found online in the Supporting Information section

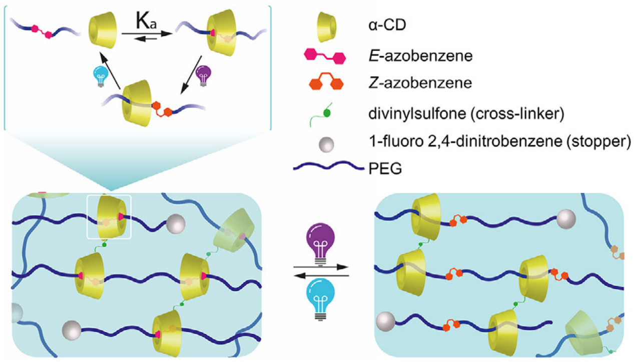

Figure 1. Concept of the photoswitchable slide-ring gels using azobenzene-containing poly(rotaxanes).

reversibly alter the sliding dynamics in situ in response to light (Figure 1). To develop these photoswitchable SRGs, we synthesized azobenzene-containing copolymers that were threaded with α-CD prior to network formation. In the *E* configuration, the azobenzenes form stable host–guest inclusion complexes with α-CD,[15] immobilizing the slide-ring cross-links. Upon photoconversion to the *Z* isomer, complex formation is no longer favorable[16–18] and the α-CD is released from its fixed position on the polymer backbone, enhancing the sliding dynamics.

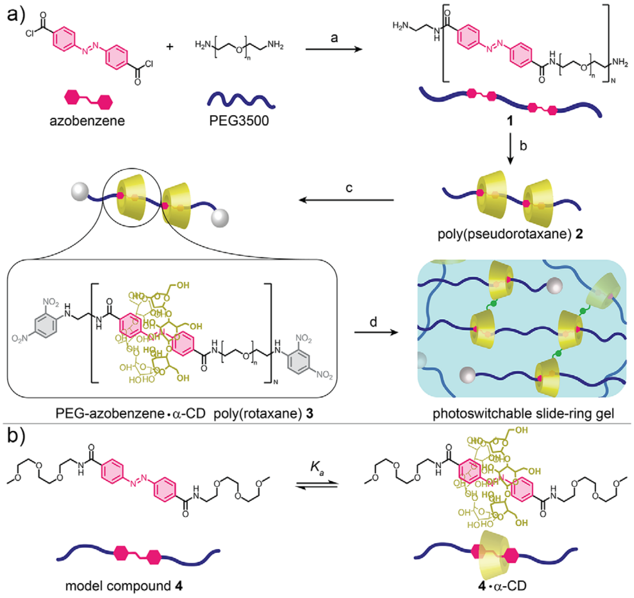

Figure 2. Synthesis of photoswitchable SRGs: a) Synthetic pathway towards the PEG-azobenzene poly(rotaxane) **3** and the gelation to obtain photoresponsive SRGs: a. TEA, CH_2Cl_2, r.t., then ethylene diamine; b. α-CD, H_2O, 80 °C; c. 1-fluoro-2,4dinitrobenzene, DMF, r.t.; d. divinylsulfone, 0.1 M $NaOH_{(aq)}$. b) Interaction of the model compound **4** with α-CD.

Results and Discussion

Conventionally, CD-based SRGs are synthesized through direct threading of the CD macrocycles onto the polymer backbone and subsequent cross-linking of disparate CDs in the system. However, in this setup, there is no region of the polymer backbone that is more or less favorable for sliding. Therefore, we designed a polymer with supramolecular guests for α-CD, namely azobenzene moieties, as a strategy to control sliding dynamics in CD-based SRGs.

Azobenzenes are among the most widely used photochromes due to their fast, reversible and robust photoisomerization that causes a change in shape and polarity of the molecule. Going from the *E* to the *Z* isomer, azobenzenes switch from a planar, nonpolar structure to a non-planar one with a dihedral angle of ~60° and an increased dipole moment equal to 3 Debye.[17] The underlying molecular changes also affect their supramolecular binding with CD. In the *E* configuration, azobenzene can fit within the inner cavity of α-CD forming a 1:1 host–guest complex, driven by hydrophobic interactions.[17] The more polar *Z* isomer adopts a configuration that does not fit perfectly within the cavity of the α-CD, substantially decreasing the binding affinity.[15–17] In this context, we hypothesized that azobenzene-based polymers within SRGs would provide a handle to modulate α-CD sliding dynamics in situ with light.

Our synthetic pathway started with the polycondensation of azodibenzoyl dichloride and an amino-telechelic poly(ethylene glycol) (PEG, 3.5 kDa) in the presence of triethylamine (TEA, Figure 2a, step a). After purification via extraction, polyamide **1** was obtained, which consisted of azobenzenes equally spaced between PEG blocks (Figure S1).[19] Two different batches were synthesized and yielded molecular weights of M_n ~24.5 and 21.0 kDa, corresponding to ~7 and ~6 azobenzene–PEG repeating units (RU) (MW_{RU} = 3736 g mol^{-1}, Figures S23, S25, Table S1). These molecular weights were confirmed by MALDI-ToF (Figures S27,S28). The obtained polyamide **1** was then threaded with α-CD to obtain a poly(pseudorotaxane) **2** (Figure S2) by adapting literature protocols (Figure 2a, step b).[20] The ^{1}H NMR spectrum revealed an α-CD/azobenzene ratio of 10, which was expected, due to the large excess of the macrocycle (Figure S2). In the final step, the ends of the CD-threaded poly(pseudorotaxane) **2** were capped with 1-fluoro-2,4-dinitrobenzene (DNFB) to form the CD-threaded poly(rotaxane) **3** (Figure 2a, step c).[21] The crude product was purified via dialysis for 2 days using a molecular weight cut-off of M_n = 6–8 kDa to yield poly(rotaxane) **3**.[22] Poly(rotaxane) **3** was designed to enable subsequent figure-of-eight cross-linking and SRG formation via the addition of divinylsulfone, which should react with free hydroxyl groups on the threaded α-CDs (Figure 2a, step d).

The molecular structure of the final poly(rotaxane) **3** was confirmed by ^{1}H NMR spectroscopy (Figures 3, S3). The successful polycondensation was verified by the formation of the amide group, which showed a proton signal at δ = 8.77 ppm (green, Figure 3a). Additionally, respective proton signals of the PEG repeating units appeared at δ = 3.56 ppm (blue, Figure 3a).

As expected, the azobenzene proton signals appeared in the aromatic region showing two doublets at δ = 8.14

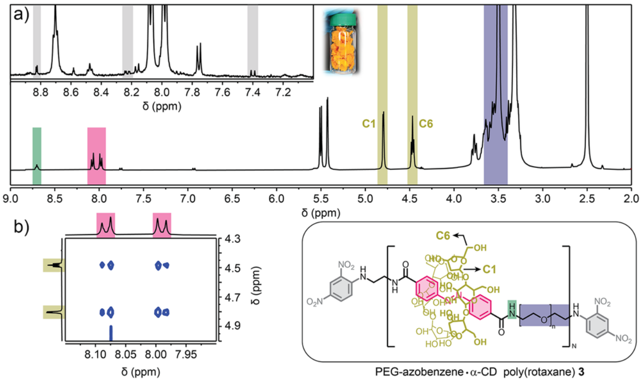

Figure 3. a) ^{1}H NMR spectra of poly(rotaxane) **3**, recorded in DMSO-d_6. Inset shows a magnification of the aromatic region, containing signals associated with the stopper. b) NOESY cross-peaks between the azobenzene protons of the poly(rotaxane) **3** and the C1 and C6 protons of the α-CD macrocycle.

and 8.04 ppm (pink, Figure 3a). Various signals belonging to the α-CD were also present (δ = 5.60–4.40 ppm), and the highlighted proton signals at δ = 4.80 and 4.50 ppm were assigned to the anomeric proton in C1 position and the hydroxyl group in C6 position of the glucose unit, respectively (yellow, Figure 3a). The presence of α-CD signals in the spectrum combined with the signals at δ = 8.82, 8.58, and 7.39 ppm corresponding to the three non-equivalent hydrogens of the dinitrobenzyl group (grey, Figure 3a) confirmed that the capping reaction was successful and the α-CD macrocycles were threaded onto the polymer chain.

Further evidence for the threading of α-CD onto the azobenzene polymer was provided by NOESY measurements (Figures 3b, S4). If threading occurs, azobenzene proton signals in proximity to the α-CD should experience a nuclear Overhauser effect (NOE). In the respective 2D spectrum (Figure 3b), cross-sectional peaks were found between the azobenzene protons and the C6 hydroxyl group as well as the anomeric proton at the glycosidic bond in C1 position, confirming proximity between these two molecular residues and thus threading in the poly(rotaxane) state.

The molecular weight of poly(rotaxane) **3** was determined via GPC and increased from M_n ~24.5 to 38.5 kDa and from M_n ~21.0 to 31.7 kDa, respectively, for the two consecutive batches (Figures S23–26, Table S1). Between the unthreaded polyamides **1** and polyrotaxanes **3**, this gave a mass difference of 14.0 and 10.7 kDa (Table S1). Based on the molecular weight of α-CD being MW = 972.85 g mol^{-1}, this indicated that an average of ~14 and ~11 macrocycles were threaded onto poly(rotaxane) **3**, respectively for the two batches. Using the degree of polymerization, this corresponded to an α-CD/azobenzene ratio of 2.0 and 1.8. These ratios were confirmed by ^{1}H NMR integration, which gave similar ratios of 2.4 and 1.8, respectively (Table S1). Since the second batch of polyrotaxane **3** (31.7 kDa) showed the best agreement for the α-CD/azobenzene ratio between the GPC and NMR measurements (1.8), this batch was used for the gelation experiments.

For the sliding motion to be modulated by irradiation, it is imperative that the α-CD macrocycles interact with the azobenzene units in the backbone of the polymer. To verify this supramolecular host–guest interaction, we first synthesized a model compound **4** to structurally simulate the azobenzene embedded in a PEG chain (Figure 2b). Model compound **4** was fully characterized by ^{1}H NMR spectroscopy. Interestingly, in DMSO-d_6 4% of the *Z*-isomer were present, whereas in CDCl$_3$, only the *E*-isomer was detected (Figures S5–S16).

The binding of α-CD with **4** was assessed using circular dichroism spectroscopy, exploiting the induced chirality of the macrocycle on the achiral guest **4** (Figure 4a, b).[23] The absorption spectrum of **4** showed the characteristic features of the azobenzene moiety, that is, the intense band in the UV region assigned to the π—π^* transition, and the weaker n—π^* band around 450 nm (Figure 4a). As expected, no circular dichroism signal was detected. Upon adding excess α-CD, significant circular dichroism signals were observed corresponding to the absorption bands of the azobenzene unit, as a consequence of the induced chirality from the chiral α-CD (Figure 4b).These results support the ability to form α-CD–azobenzene complexes along PEG polymers.[24] The binding of **4** with α-CD was also confirmed in an ^{1}H NMR experiment, where the presence of 1 eq of the macrocycle led to a downfield shift of the azobenzene proton signal (Figure S17).[25] The binding affinity for this complex was quantitatively measured to be K_a = 120 M^{-1} via isothermal titration calorimetry (ITC, Figure S29).

Repeating the experiment with polyamide **1** yielded analogous results. Much like **4**, polymer **1** on its own did not exhibit chirality in the circular dichroism, and the absorption spectrum originated from the incorporated azobenzene units (Figure 4c, d). In the presence of α-CDs, however, the resulting circular dichroism spectrum exhibited signals at the same wavelengths as the absorption of azobenzene, indicating that the macrocycles encapsulate the azobenzene units on the polymer. For the binding of α-CD to **1**, an apparent binding constant of K_a = 454 M^{-1} was measured via ITC (Figure S29). Overall, these findings confirmed that α-CD was able to bind to the azobenzene units of **1** and should therefore enable the immobilization of macrocycles within the polymer network.

To enable reversible interactions between azobenzene and α-CD in the polymeric state, we attempted to photoisomerize the azobenzene units in polymer **1**, which should weaken their interaction with α-CD. For this, absorption and circular dichroism spectra of polyamide **1** were recorded in the presence of excess α-CD before and after light irradiation at λ = 365 nm (Figure 4c, d). Notably, the signal in the circular dichroism spectrum decreased upon irradiation, suggesting a reduction of the induced chirality, indicative of the release of the *Z* azobenzene from the α-CD cavity. The analogous experiment was performed with poly(rotaxane) **3**. The circular dichroism signal of poly(rotaxane) **3** was less intense than the ones of **4** and **1** (Figure 4e, f). This was likely an effect of the different α-CD concentrations, since an excess of α-CD was used for **4** and **1**, while for poly(rotaxane) **3**, the α-CD content was restricted to the macrocycles threaded

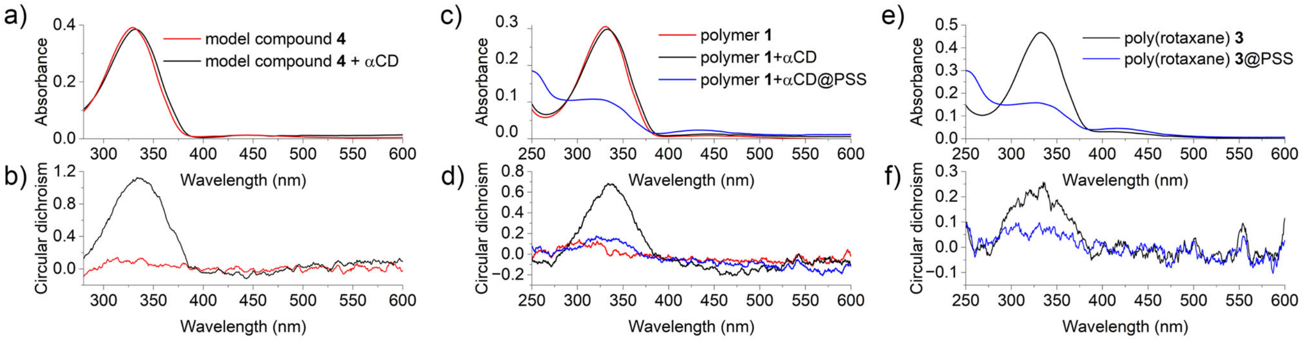

Figure 4. Absorption spectra (a,c,e) and circular dichroism (b,d,f) recorded in 15:85 CH_3CN-H_2O of model compound **4** ($1.74{\cdot}10^{-5}$ M) in the absence (red line) and presence (black line) of excess α-CD (20 mM); of polymer **1** (0.13 mg mL^{-1}) (red line) in the presence of excess α-CD (50 mM) before (black line) and after (blue line) irradiation at $\lambda = 365$ nm until the photostationary state (PSS) is reached and of poly(rotaxane) **3** (0.13 mg mL^{-1}) before (black line) and after (blue line) irradiation at $\lambda = 365$ nm until PSS is reached.

during synthesis. Nonetheless, irradiation of **3** up to the photostationary state (PSS) led to a loss of the induced chirality signal, indicating that the α-CD macrocycles could still dissociate from the azobenzene moieties and slide along the PEG chain, even when they remained threaded on the polymer due to the presence of stoppers.

The above findings were further confirmed through UV–Vis and ^{1}H NMR irradiation experiments. For the UV–Vis experiments, model compound **4**, polymer **1** and poly(rotaxane) **3** were irradiated until the PSS was reached (Figure S30). Across the board, spectral changes characteristic of the *E* to *Z* azobenzene isomerization were observed for all species, that is, the intensity of the π—π^* band decreased, while the n—π^* band at $\lambda = 430$ nm increased (Figure S30). We also monitored the thermal back isomerization at room temperature for polymer **1** starting from the *Z* isomer, which was remarkably slow, regaining the *E* isomer only after more than 2 months (Figures S31,S32).

In the ^{1}H NMR studies, species **4**, **1,** and **3** were each dissolved in 15:85 CD_3CN—D_2O prior to light irradiation at 365 nm for 60 min (Figures S19–S21). Based on the integrals, for the three species **4**, **1**, and **3**, the fractions of *Z* isomer were estimated to be 25%, 17%, and 29%, respectively. Notably, when the irradiation of **4** was performed in DMSO-d_6, the estimated fraction of the *Z* isomer was 58%, showing a strong solvent dependence of the isomerization process (Figure S22).[26] When irradiated for 10 min at 405 nm, all three species were successfully transformed back to the *E* isomer (Figures S19–S22). Overall, these results confirm that the azobenzene units could reversibly switch from *E* to *Z* causing the α-CDs to be released from the supramolecular host–guest complex, potentially modulating the sliding dynamics in the gel state.

Having demonstrated the ability to form host–guest complexes between α-CD and azobenzene in the polymer state and that the binding behavior can be modulated via light exposure, we incorporated poly(rotaxane) **3** into networks to assemble lightresponsive SRGs. For the cross-linking reaction, we used an oxa-Michael addition between divinylsulfone (DVS) and available hydroxyl groups of the α-CD in the presence of $NaOH_{(aq)}$ as a base.[27,28] For gelation, solutions of poly(rotaxane) **3** ($M_n = 31.7$ kDa, Figure S26) were prepared in 0.1 M $NaOH_{(aq)}$ prior to the addition of DVS (3 wt%, ~5 eq per CD).

The formed SRGs (8, 12, and 16 wt%) were characterized using oscillatory shear rheology (Figure 5). Time sweeps over the first hour after initiating gelation revealed plateau moduli of G' = 140, 830, and 2650 Pa for the respective formulations (Figure 5a). Strain sweeps were performed to investigate the linear viscoelastic region (LVER) of the SRGs as well as their behavior at large amplitude oscillatory strains (LAOS). All SRGs exhibited a low strain plateau modulus and yielded at high strains (Figure 5b). With increasing polymer content of the SRGs, the yield strain decreased. All samples exhibited an overshoot in loss modulus when subjected to LAOS.[29] This feature, generally known as the Payne effect, is associated with the breakdown of substructures and can provide an estimate of the energy dissipated during the yielding process (U_d). With increasing gel concentration (8, 12, and 16 wt%), the respective energies increased as well (8, 160, and 450 kJ m^{-3}, Figure S34). Literature reports have shown that the deformation of SRGs often leads to a heterogeneous distribution of free cyclic molecules, which results in the formation of clusters prior to breaking down under LAOS.[7,30,31] Noticeably, when a strain sweep was carried out at 60 °C, no Payne peak was observed, indicating that under these conditions the macrocycles become too dynamic to create substructures during yielding (Figure S35).

Next, we performed frequency sweeps of our gels to probe their stiffness at different timescales. In all curves, the moduli increased with frequency (Figure 5c). To cover a broader frequency range, a time temperature superposition experiment was carried out with frequency sweeps between 5 °C and 60 °C (Figure S36A–B). However, the shift factors of the resulting master curve revealed two temperature regimes (T = 5–35 and 40–60 °C, Figure S36C–D), of which only the first one could be fitted using the Arrhenius model to obtain an activation energy of $E_a = 116$ kJ mol^{-1}. To ensure that TTS was applicable over the entire temperature range, a Van Gurp–Palmen plot was created. From 5 °C to 35 °C, the recorded data superimposed, making TTS applicable for this temperature range. From 40 °C to 60 °C, data did not

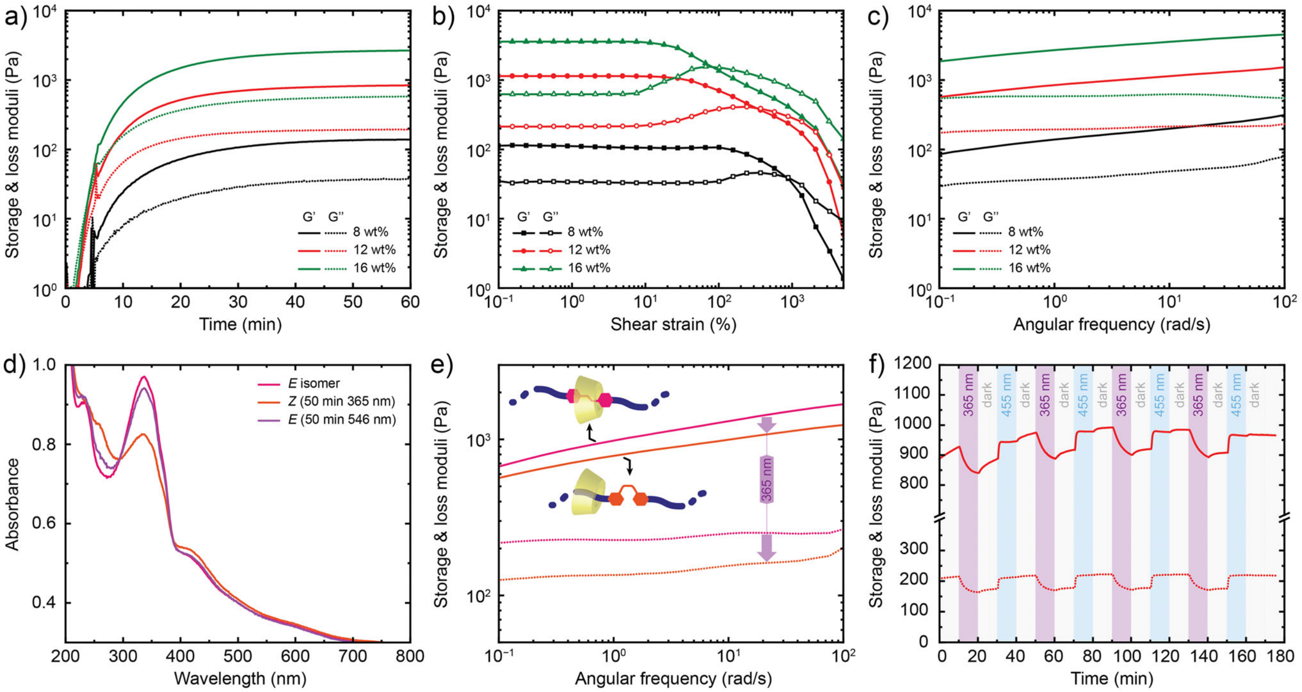

Figure 5. a) Time sweeps ($\gamma = 0.5\%$, $\omega = 10$ rad·s^{-1}), b) strain sweeps ($\gamma = 0.1\%$–5000%, $\omega = 0.5$ rad·s^{-1}), and c) frequency sweeps ($\gamma = 0.5\%$, $\omega = 1000.1$ rad·s^{-1}) of SRGs prepared in 0.1 M NaOH$_{(aq)}$ at 8 wt% (black), 12 wt% (red), and 16 wt% (green). d) UV–Vis spectra of a thin hydrogel film before (pink) and after irradiation (orange) at 365 nm light as well as after irradiation at 546 nm light (purple). e) Frequency sweeps ($\gamma = 0.5\%$, $\omega = 100$–0.1 rad·s^{-1}) of a hydrogel before (pink) and after (orange) irradiation with 365 nm light. f) time sweep ($\omega = 1$ rad·s^{-1}, $\gamma = 5\%$) consisting of 10 min interval cycles of darkness, irradiation at 365 nm, darkness, irradiation at 455 nm of the gel sample. Storage and loss moduli are depicted as straight lines (or filled symbols) and dotted lines (or hollow symbols), respectively.

superimpose, rendering TTS inapplicable due to rheologically more complex behavior. The latter could potentially be connected to the sliding transition, a temperature regime causing the macrocycles to independently slide, yet still very little is known on this phenomenon.[31] Finally, we plotted a corrected version of the TTS master curve ($T = 5$ °C to 35 °C), which showed that the moduli decreased down to angular frequencies of 0.005 rad s^{-1}, but without causing a cross-over (Figure S36F).

The frequency dependence of the moduli may be tied to the dynamics of the supramolecular host–guest complex, which at lower frequencies can contribute to the relaxation of the material (as opposed to high frequencies, where it cannot, hence, reaching a plateau modulus). This is contrary to PEG-based SRGs in the literature, where in absence of host–guest motifs along the backbone, moduli are commonly frequency-independent.[32] To check this, we measured SRGs prepared in DMSO (with NaOH), which according to ^{1}H NMR measurements of **4** and α-CD in DMSO-d_6 should be devoid of supramolecular interactions (Figure S18). Indeed, in the DMSO control gel, the moduli were frequency-independent across the measured frequency range (Figure S37).

To verify the ability of the azobenzene to isomerize also in the hydrogel, a thin film was characterized by UV–Vis spectroscopy before and after irradiation (Figure 5d). The absorption bands of the azobenzene units were recognizable in the spectrum of the hydrogel film. Upon irradiation at 365 nm the absorption peak at 335 nm decreased in intensity, indicating *E* to *Z* isomerization. Reverse *Z* to *E* isomerization occurs upon irradiation in the visible region: indeed, the absorption peak at 335 was almost completely restored under irradiation at 546 nm at room temperature.[33]

To assess the effect of isomerization on the mechanical properties of the gel, the rheology of SRGs was investigated under UV irradiation. After loading the precursor solution on the rheometer, a 1 h time sweep was followed by a frequency sweep. In the second step, the gel was irradiated with 365 nm light for 50 min prior to another frequency sweep (Figures 5e, S38). Upon sample irradiation, the storage modulus at 10 rad s^{-1} decreased from G' = 1030 to 800 Pa, while the loss modulus fell from G“” = 240 to 140 Pa. This drop in moduli was preserved across the entire frequency range (Figure 5e) and was also observed in the respective strain sweeps (Figure S39).

Finally, to test the reversibility of the isomerization and hence the sliding dynamics, the photoresponsiveness of the SRG was assessed via a time sweep experiment where the sample was subjected to 10 min intervals of irradiation at 365 nm, darkness, and irradiation at 455 nm (Figure 5f). The dynamic moduli indicated that the reversible isomerization could be repeated over multiple cycles, where the network was weakened first and then stiffened through the reversible photoswitching of the azobenzenes in the backbone. Noticeably, irradiation of a DMSO control gel did not exhibit photoresponsive stiffness, which was in agreement with previous experiments indicating that DMSO as a good

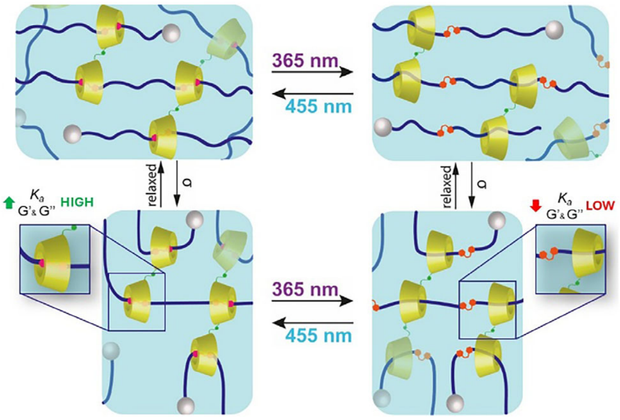

Figure 6. Mechanism for the modulation in sliding motion of photo-responsive SRGs. Top left represents the situation in the dark when the azobenzene unit is in the *E* configuration and the gel is relaxed. Here, the association between the azobenzene and the α-CD is strong, therefore when shear stress is applied higher moduli are displayed. Upon irradiation at 365 nm (top right) the azobenzene isomerize to the *Z* configuration, which does not bind to the CD macrocycle having a lower K_a. As a result, both moduli decrease proving a reduction in material stiffness.

solvent for both azobenzenes and α-CDs weakened their supramolecular interaction, emphasizing the need for an aqueous environment (Figure S40). Further to this, a simple swelling experiment of two bulk gels showed that when the gel was irradiated continuously at 365 nm light, a higher degree of swelling was obtained than for a gel that was kept in the dark (Figure S41). This is in line with a softer gel being able to swell more.

Finally, it should be noted that although both the spectrophotometric and the rheological results (Figure 5d–f) collectively demonstrate the successful photoinduced azobenzene isomerization within the gel and its impact on the material's mechanical properties, it can only be compared on a qualitative and not quantitative level due to the inherently different experimental setups and technical constraints (see SI for details).

Nonetheless, our results highlight that in $NaOH_{(aq)}$ the hydrophobic azobenzene units favor association with α-CDs, which in turn enables the photo-responsive behavior, the modulation of the sliding dynamics and hence, the material stiffness by light.

Conclusion

In summary, we demonstrated that by synthesizing a guest containing PEG-based polymer, we were able to fabricate SRGs that show dedicated interactions at defined sites along the polymer backbone. We further showed that reversible switching of this interaction could be used to alter the sliding motion of the CDs on the polymer with discernible implications for the stiffness of the material (Figure 6). In the dark, the *E* isomer, which is the most thermodynamically stable configuration of the azobenzene unit, binds with the α-CD. The host–guest complex formation inhibits the ability of the macrocycle to slide along the polymer chain, increasing both the storage and loss moduli of the resulting SRG. This is analogous to the fixed-state, which has been described in cation-templated systems reported by Ghiassinejad et al.[2]

Upon irradiation at 365 nm, the *E*-azobenzene converts to the *Z* isomer displacing the α-CD, which cannot bind with the *Z* isomer. Consequently, the threaded macrocycles now reside on the PEG chain allowing for free movement along the backbone. Hence, both storage and loss moduli decrease in this free state. Irradiation of the sample at 455 nm induces back photoisomerization, the host–guest complexes reengage, restoring both moduli to their initial values. Importantly, this is the first CD-based material of its kind, where the stiffness is altered through a reduction in slide-ring mobility and not through a change in crosslinking density, as shown in other reports.[16,34,35] Uniquely, we have demonstrated that supramolecular interactions of the macrocycles to the backbone—enabled by the incorporation of photoactive units—can modulate the pulley effect, which represents a key feature of SRGs. In the *E* state, the strong affinity between the polymer and α-CD impedes the sliding motion, blocking the pulley. In the *Z* form, however, azobenzenes do not bind the α-CDs allowing the PEG chains to slide and dissipate stress.

Based on the present platform, we aim to expand our efforts in the field of SRGs in the future, providing further mechanistic insights into the unique topology of SRGs by using different recognition units, macrocycles, and stimuli. Similar polymers as building blocks can be designed to create SRGs with defined backbone affinities and polycondensation reaction represents a straightforward approach for preparing such materials with potential applications in the biomedical field, as coatings or high-performance hydrogel materials.

Supporting Information

The authors have cited additional references within the Supporting Information.[36–41]

Acknowledgements

This work was supported by an SNSF Ambizione Grant (PZ00P2_202141; S. M.) and by the Italian Ministry of University and Research (PRIN grant 201732PY3X; S. S.). The authors would like to thank the NMR Service at the Department of Chemistry and Applied Biosciences (D-CHAB) at ETH Zurich. The authors further would like to acknowledge Caterina Bellatreccia for creating the sketch drawings of the graphical abstract.

Open access publishing facilitated by Eidgenossische Technische Hochschule Zurich, as part of the Wiley - Eidgenossische Technische Hochschule Zurich agreement via the Consortium Of Swiss Academic Libraries.

Conflict of Interests

The authors declare no conflict of interest.

Data Availability Statement

The data that support the findings of this study are openly available in ETH Research Collection at https://doi.org/10.3929/ethz-b-000742913.

Keywords: Azobenzene • Cyclodextrins • Photochemistry • Slide-ring gels • Sliding dynamics

---

[1] K. Ito, *Chem. Pharm. Bull.* **2017**, *65*, 326–329.
[2] S. Ghiassinejad, A. Kumar Sharma, C.-A. Fustin, E. Van Ruymbeke, *Chem. Mater.* **2024**, *36*, 8311–8322.
[3] R. Du, T. Bao, D. Kong, Q. Zhang, X. Jia, *ChemPlusChem* **2024**, *89*, e202300706.
[4] T. Murakami, B. V. K. J. Schmidt, H. R. Brown, C. J. Hawker, *J. Polym. Sci. A1.* **2017**, *55*, 1156–1165.
[5] H. Sogawa, T. Tsutsuba, N. Sakiyama, T. Ikeda, T. Takata, *Macromol. Rapid Commun.* **2021**, *42*, 2000639.
[6] L. Yang, Y. Wang, G. Liu, J. Zhao, L. Cheng, Z. Zhang, R. Bai, Y. Liu, M. Yang, W. Yu, X. Yan, *Angew. Chem. Int. Ed.* **2024**, *63*, e202410834.
[7] L. Chen, Y. Liu, W. You, J. Wang, Z. He, H. Mei, X. Yang, W. Yu, G. Li, F. Huang, *Angew. Chem. Int. Ed.* **2025**, *64*, e202417713.
[8] Q. Li, Y. Yang, S.-M. Yu, Z. Wu, J. Xing, Q. Lin, Y. Miao, H. Wang, D.-W. Zhang, W. Wang, Z.-T. Li, Y.-X. Xu, *ACS Appl. Mater. Interfaces* **2024**, *16*, 48342–48351.
[9] Y. Okumura, K. Ito, *Adv. Mater.* **2001**, *13*, 485–487.
[10] G. Fleury, G. Schlatter, C. Brochon, C. Travelet, A. Lapp, P. Lindner, G. Hadziioannou, *Macromolecules* **2007**, *40*, 535–543.
[11] L. Jiang, C. Liu, K. Mayumi, K. Kato, H. Yokoyama, K. Ito, *Chem. Mater.* **2018**, *30*, 5013–5019.
[12] M. Ogawa, A. Kawasaki, Y. Koyama, T. Takata, *Polym. J.* **2011**, *43*, 909–915.
[13] K. Yamamoto, R. Nameki, H. Sogawa, T. Takata, *Angew. Chem. Int. Ed.* **2020**, *59*, 18023–18028.
[14] L. F. Hart, W. R. Lenart, J. E. Hertzog, J. Oh, W. R. Turner, J. M. Dennis, S. J. Rowan, *J. Am. Chem. Soc.* **2023**, *145*, 12315–12323.
[15] Y.-L. Zhao, J. F. Stoddart, *Langmuir* **2009**, *25*, 8442–8446.
[16] N. Liubimtsev, Z. Zagradska-Paromova, D. Appelhans, J. Gaitzsch, B. Voit, *Macromol. Chem. Phys.* **2023**, *224*, 2200372.
[17] D. Wang, W. Zhao, Q. Wei, C. Zhao, Y. Zheng, *ChemPhotoChem* **2018**, *2*, 403–415.
[18] S. Tamesue, Y. Takashima, H. Yamaguchi, S. Shinkai, A. Harada, *Angew. Chem. Int. Ed.* **2010**, *49*, 7461–7464.
[19] H. Zhao, T. Hong, M. Lan, W. Wang, S. Zheng, B. Liu, *J. Nanosci. Nanotech.* **2013**, *13*, 1295–1299.
[20] A.-M. Resmerita, K. I. Assaf, A. I. Lazar, W. M. Nau, A. Farcas, *Eur. Polym. J.* **2017**, *93*, 323–333.
[21] A. Harada, J. Li, M. Kamachi, *Nature* **1992**, *356*, 325–327.
[22] This cut-off was chosen to be well above the molecular weight of the α-CD and any other organic reagents to ensure complete removal of any low-molecular weight impurities.
[23] W. Qi, C. Ma, Y. Yan, J. Huang, *Curr. Opin. Colloid Interface Sci.* **2021**, *56*, 101526.
[24] J. Royes, C. Courtine, C. Lorenzo, N. Lauth-de Viguerie, A.-F. Mingotaud, V. Pimienta, *J. Org. Chem.* **2020**, *85*, 6509–6518.
[25] This shift was only observed when aqueous media were used. In the strongly polar solvent DMSO-d_6, no apparent shift of the azobenzene protons was observed, signifying a weakening of the supramolecular host–guest interactions (Figure S18).
[26] It should be noted that these values are just estimations and do not equate to the PSS ratio, which due to reduced spectral resolution, imperfect mixing and light diffusion can likely not be reached in the NMR tubes.
[27] A. A. M. Shimojo, A. M. B. Pires, R. Lichy, M. H. A. Santana, *J. Braz. Chem. Soc.* **2015**, *26*, 506–512.
[28] J. Morales-Sanfrutos, F. Lopez-Jaramillo, M. Elremaily, F. Hernández-Mateo, F. Santoyo-Gonzalez, *Molecules* **2015**, *20*, 3565–3581.
[29] *Carbon-Based Nanofillers and Their Rubber Nanocomposites*, (Eds.: S. Yaragalla, R. K. Mishra, S. Thomas, N. Kalarikkal, H. J. Maria), Elsevier, Amsterdam **2019**.
[30] Y. Shinohara, K. Kayashima, Y. Okumura, C. Zhao, K. I. Y. Amemiya, *Macromolecules* **2006**, *39*, 7386–7391.
[31] K. Ito, *Polym. J.* **2012**, *44*, 38–41.
[32] T. Murakami, B. V. K. J. Schmidt, H. R. Brown, C. J. Hawker, *Macromolecules* **2015**, *48*, 7774–7781.
[33] Interestingly, when a thin hydrogel film was irradiated for 50 min at 365 nm to convert to the *Z* isomers, subsequent heating of the sample at 60 °C for 4 h resulted in complete thermal back isomerization to the *E* isomers (providing an additional handle for re-isomerization, Figure S33).
[34] T. Sakai, H. Murayama, S. Nagano, Y. Takeoka, M. Kidowaki, K. Ito, T. Seki, *Adv. Mater.* **2007**, *19*, 2023–2025.
[35] D. Tian, W. Ma, L. Zheng, K. Jiang, H. He, R. Sun, *ACS Appl. Polym. Mater* **2023**, *5*, 8641–8649.
[36] M. Montalti, A. Credi, L. Prodi, M. T. Gandolfi, *Handbook of Photochemistry*, CRC Press, Boca Raton, **2006**.
[37] S. Keller, C. Vargas, H. Zhao, G. Piszczek, C. A. Brautigam, P. Schuck, *Anal. Chem.* **2012**, *84*, 5066–5073.
[38] T. H. Scheuermann, C. A. Brautigam, *Methods* **2015**, *76*, 87–98.
[39] C. A. Brautigam, H. Zhao, C. Vargas, S. Keller, P. Schuck, *Nat. Protoc.* **2016**, *11*, 882–894.
[40] C. A. Brautigam, in *Methods in Enzymology*, Elsevier, Amsterdam **2015**, pp. 109–133.
[41] R. Meusinger, *Anal. Bioanal. Chem.* **2024**, *416*, 5217–5219.

Manuscript received: March 28, 2025
Revised manuscript received: June 30, 2025
Accepted manuscript online: July 03, 2025
Version of record online: July 20, 2025